Near Surface Geophysics

EAGE EUROPEAN ASSOCIATION OF GEOSCIENTISTS & ENGINEERS

Near Surface Geophysics, 2019 doi: 10.1002/nsg.12042

Imaging scours in straightened and braided gravel-bed rivers with ground-penetrating radar

Emanuel Huber*, Birte Anders and Peter Huggenberger

Applied and Environmental Geology, University of Basel, Basel, Switzerland

Received October 2018, revision accepted April 2019

ABSTRACT

The genesis of alternate gravel bars in straightened rivers and braided rivers is closely coupled to the formation of scours. Scours can lead to riverbank failure, initiate lateral river dynamics and strongly impact the interaction between surface and subsurface flow and transport. It is, therefore, critical to account for scours in the design of flood protection measures. However, there is still little knowledge on the formation and characteristics of such scours, especially on the dynamic relationship between the riverbed morphology and the scours. Bathymetric riverbed surveys conducted at medium to low discharge may underestimate the real scour sizes and shapes if scours filled with sediments during waning discharge. Furthermore, the literature suggests that gravel bars and scours can jointly migrate on the riverbed, resulting in cut-and-fill sedimentary structures in the near subsurface. These cut-and-fill structures cannot be observed from the surface. We investigate with ground-penetrating radar the presence of scour fills below the riverbed of two gravel-bed rivers and study any indications of bar and scour migration. Thus, two ground-penetrating radar surveys were conducted, one on the emerged part of an alternate bar of the channelized Alpine Rhine River (Switzerland) and the other on a flat gravel surface in a braided reach of the Tagliamento River (Italy) that is near the pristine state. At both sites, a scour fill could be clearly identified below a 2-m-thick sediment layer. The imaged part of the scour of the Alpine Rhine River ($30 \times 100 \times 4.5$ m) is located at the front end of the gravel bar next to the riverbank. This scour was only partially imaged by ground-penetrating radar and is in reality significantly deeper and larger. The scour of the Tagliamento River ($20 \times 30 \times 2.5$ m) shows a clear internal structure consisting of inclined, planar cross-beds that merge tangentially with the lower-bounding erosional surface of the scour. At the light of the literature, we compare these two scours in terms of sedimentary processes resulting from the complex interplay between scours and gravel bars. The study findings offer a promising research avenue on the dynamic relationship between discharge, sediment transport, scour and bar formation and migration.

Key words: Geotechnical, Ground-penetrating radar, Shallow subsurface.

INTRODUCTION

In the last centuries, rivers were channelized and straightened to mitigate flooding by increasing discharge and sediment transport. Instead of the expected flat riverbeds, alternate bars appeared in many straightened gravel-bed rivers (e.g. Grebenau 1870). Alternate bars are elongated bedforms formed at high discharge that alternatively lie on the left and right river sides and emerge at low discharge as displayed in the aerial photograph in Fig. 1(b). Laboratory experiments

*E-mail: emanuel.huber@unibas.ch

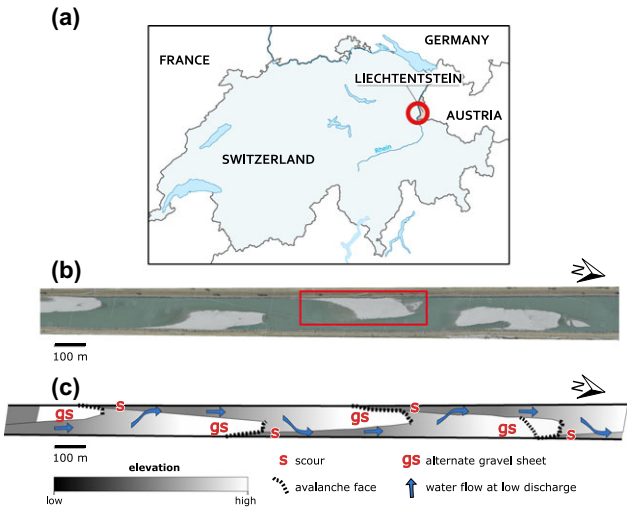

Figure 1 Site 1. (a) Location of the Alpine Rhine River site in Switzerland. (b) Aerial photograph of the Alpine Rhine River with alternate gravel sheets (bars). The red box indicates the selected gravel sheet (coordinates 538,918; 5,219,325 WGS84 UTM 32T). (c) Morphological interpretation of (b). Adapted from Huber, Anders and Huggenberger (2018).

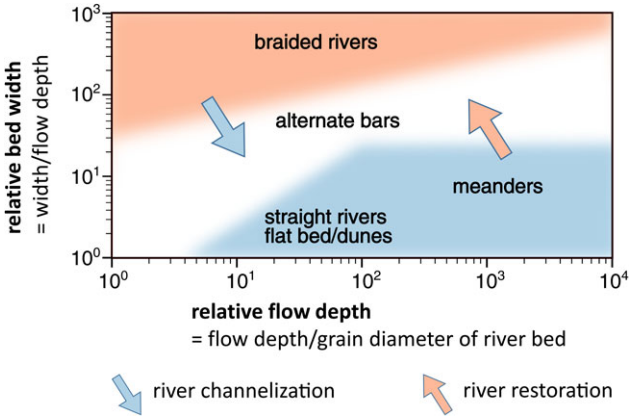

Figure 2 River morphology as a function of relative flow depth and relative bed width (adapted from Marti and Bezzola 2005). The blue and red arrows indicate the potential change of river morphology induced by river channelization and restoration.

showed that each alternate bar is associated with a scour upstream close to the riverbank as illustrated in Fig. 1(c) (see also Ikeda 1984; Pyrce and Ashmore 2003; Bankert and Nelson 2018). Alternate bars can induce lateral erosion by deviating the flow towards the riverbanks. Therefore, many studies interpreted alternate bars as an initial state of braided rivers (Parker 1976; Ashmore 1985; Hundey and Ashmore 2009; Kleinhans and van den Berg 2011). Gravel-bed, braided rivers are also characterized by bars associated with confluence scours (Siegenthaler and Huggenberger 1993; Huggenberger and Regli 2006).

The formation of alternate bars is controlled by complex feedbacks between the riverbed dynamics and the turbulent flow structure (Best 1993; Kleinhans and van den Berg 2011). It was observed that alternate bars and their associated scours appear under specific slope, channel width and grain size settings as shown in the diagram in Fig. 2 (Jäggi 1984; Marti and Bezzola 2005). Therefore, the channelization of braided rivers or the restoration (e.g. widening) of rivers that are originally free of alternate bars can change the relative bed width and flow depth such that alternate gravel bars and their scours appear. This setting change is represented by the arrows in Fig. 2. River restoration generally aims to re-establish a more natural sediment dynamics and therefore to favour the formation of gravel bars and indirectly of scours. The latter are critical for the stability of river embankments (Jäggi 1984) and therefore the maximum scour depth is a key parameter for the design of reliable flood protection measures.

At high discharge, alternate bars and their associated scours can migrate downstream up to several hundreds of metres (Adami, Bertoldi and Zolezzi 2016). During discharge recession, the scours can fill with sediments such that they are no more visible from the surface at low discharge (Storz-Peretz and Laronne 2013). Because riverbed bathymetric surveys are generally conducted at medium to low discharge, they may not capture the real scouring depth and extent. Salter (1993) already recognized the significance of scours for the sedimentary records. Because scours are located at the lowest positions and can migrate, they can rework significant parts of the deposits and have the largest chance of being preserved in the sedimentary records (Salter 1993; Siegenthaler and Huggenberger 1993; Huber and Huggenberger 2015).

Many studies showed that the sedimentary structure of scour fills generally consists of alternating open-framework–bimodal couplet cross-beds (e.g. Siegenthaler and Huggenberger 1993; Jussel, Stauffer and Dracos 1994; Beres *et al.* 1999; Bayer *et al.* 2011). An open-framework–bimodal couplet gravel is a gravel consisting of bimodal gravel at the base and open-framework gravel at the top. An open-framework gravel has a narrow range of grain sizes (i.e. a well-sorted gravel) in which the pore space is free of sand and silt. Bimodal gravel consists of a well-sorted gravel framework in which the pores are filled with a well-sorted medium sand. A transition from bimodal to open-framework gravel is generally marked by a sharp boundary between the pores of the bimodal gravel filled with sand and the open pores of the open-framework

gravel. The grain size usually fines upward from the bimodal to the open-framework gravel (coarsest grain size at the base and finest at the top).

The open-framework gravel is much more permeable than the other deposits (up to three orders of magnitude). Scour fills consisting in open-framework–bimodal couplets strongly impact subsurface flow and transport (Huber and Huggenberger 2016) and therefore river water–groundwater exchange (Huggenberger *et al.* 1998). The latter is highly relevant in the riverbank filtration process used for drinking water supply. Furthermore, the ecological impact of scour fills, for example, on benthic macroinvertebrate abundance, is still poorly known (Huggenberger and Regli 2006).

To our knowledge, the sedimentological comparison between scours associated with alternate bars and confluence scours found in braided rivers has not yet been drawn. Furthermore, there is little knowledge on the sedimentary processes related to the formation and migration of scours at high discharge (Claude *et al.* 2014) and on the scour footprints left in the sedimentary records (Ashmore and Gardener 2008). The relationship between bars, scour formation and scour fills is still almost unexplored (Huber and Huggenberger 2015).

Ground-penetrating radar (GPR) can contribute to a better understanding of the sedimentary structures below the riverbed. Many studies compared GPR data with excavated vertical exposures in gravel carries and showed that GPR is strongly indicated to portray the erosional lower-bounding surfaces of buried scours as well as their internal structure (e.g. Huggenberger 1993; Huggenberger, Meier and Pugin 1994; Beres *et al.* 1995, 1999; Asprion and Aigner 1997, 1999; Heinz and Huggenberger *et al.* 1998; Heinz and Aigner 2003; Kostic and Aigner 2007; Bayer *et al.* 2011). Although GPR cannot image all the sedimentary details, it has been demonstrated that the reflection patterns are good indicators of the sedimentary structures (e.g. Dam and Schlager 2000).

The relative dielectric permittivity has a strong impact on the electromagnetic wave propagation and reflection. While air and most dry geologic media have a low relative dielectric permittivity (<10), water has a relative dielectric permittivity around 80 (Davis and Annan 1989). Therefore, the relative dielectric permittivity of gravel deposits is controlled mainly by their water content, which strongly depends on the porosity in the saturated zone and on the water saturation in the unsaturated zones. Both are related to the subsurface heterogeneity, that is, to spatial variations of the sediment grain type, composition, shape and orientation (Huggenberger 1993; Dam and Schlager 2000; Neal 2004). A scour is characterized by an erosional lower-bounding surface cut into the underlying deposits by high-velocity flows. The scour can be filled with sediments that contrast in terms of grain size distribution, orientation etc. with the underlying sediments. Therefore, erosional lower-bounding surfaces often mark an abrupt change in sedimentological texture (sediment size, orientation and composition), resulting in a change of water content and producing a reflection of the GPR wave (Huggenberger 1993).

In this contribution, we investigate with GPR the presence of scour fills in two gravel-bed rivers and study any indications of bar and scour migration. The imaged scour fills are put into relation with the surface morphology (e.g. gravel bars) and the type of scouring processes are inferred from the data. GPR data were collected at low discharge on the riverbeds of the Alpine Rhine River (NE Switzerland), a straightened river with alternate bars, and of the Tagliamento River (NE Italy), a gravel-bed, braided river in near pristine state. This publication is based on some results presented in Huber, Anders and Huggenberger (2018).

In the following, we use the sedimentological term 'gravel sheet' instead of the morphological term 'bar' (see also Siegenthaler and Huggenberger 1993, p. 149), because this study focuses on the sedimentary processes related to the dynamic interplay between gravel sheets and scours.

STUDY SITES

We selected two sites to collect a series of GPR data. The first site is a 200 × 60 m alternate sheet at 43.5 km of the Alpine Rhine River up to Lake Constance in Switzerland (Figs 1 and 3) and the second site is located on top of a flat gravel surface in a braided reach of the Tagliamento River (Northeast Italy).

Alpine Rhine River site

The Alpine Rhine River has a 6100 km^2 large catchment and flows after 90 km into the Lake Constance. This gravel-bed river has a pluvio–nival regime with the largest discharges in June caused by snowmelt. At the river mouth in Lake Constance, the mean discharge is 230 m^3/s and the 100-year discharge is 3100 ± 200 m^3/s (Zarn 2008; a 100-year discharge has a 1% probability of occurring in any year). Over the past 150 years, the Alpine Rhine River was systematically trained and channelized to increase discharge capacity and sediment transport. Because of the joint effect of river training and gravel extraction, the riverbed predominantly deepened in the last century.

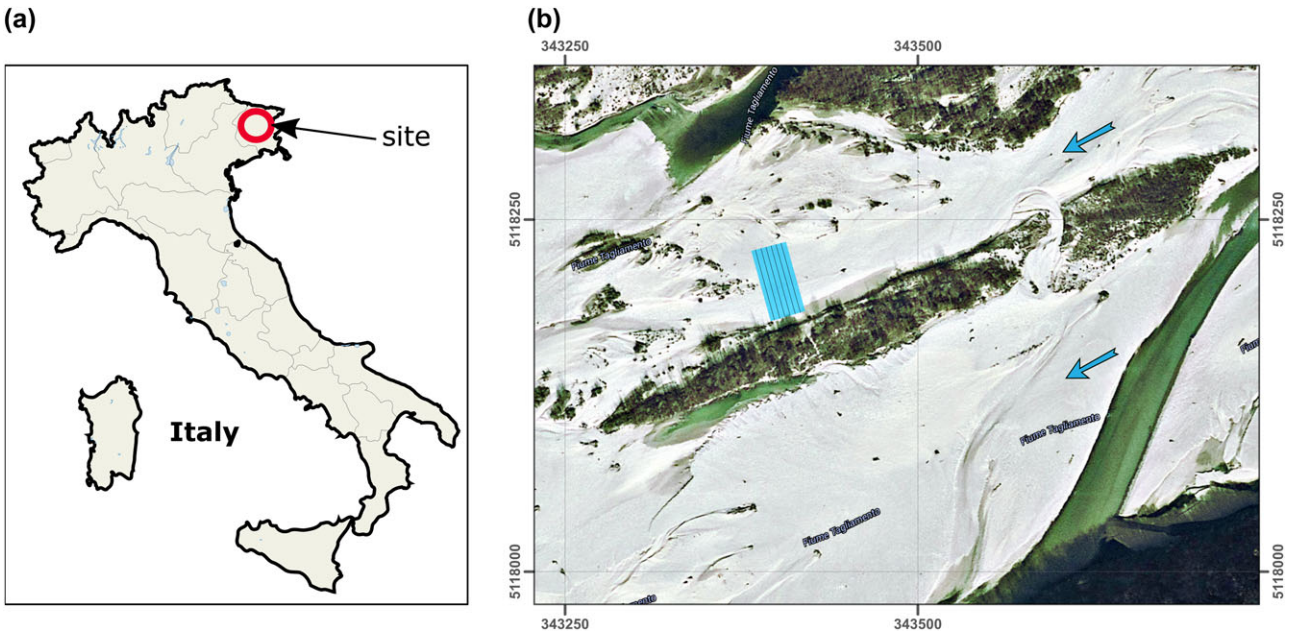

Figure 3 Site 2. (a) Location of the selected reach of the Tagliamento River in Italy. (b) Location of the ground-penetrating radar survey (the blue rectangle) on the riverbed of the Tagliamento River (coordinates: 236,388; 5,118,308 WGS 1984 UTM 33N). The blue arrows indicate the general flow direction.

Figure 1(b) shows the gravel sheet selected for the GPR survey (km 43.5, coordinates: 538,918; 5,219,325 WGS84 UTM 32T). The gravel sheet was selected because it was well preserved and the reach was straight and therefore free of any bend effects. At this location, the riverbed has a trapezoidal cross-section and is about 100 m wide. There, the riverbed deepened by approximately 4 m (degradation) since 1940 and model predictions show that the degradation will continue at a moderate rate in a near future (Zarn 2008). Alternate gravel sheets dominate between the Landquart's confluence (km 23.3) and the Ill's confluence (km 65.0). Adami *et al.* (2016) studied with Landsat images the gravel sheet dynamics within this reach between 1984 and 2011. While in some sub-reaches most of the alternate gravel sheets are stationary, the gravel sheets from the sub-reach corresponding to km 43.5 (study site) showed the largest downstream migration rate (up to 300 m per flood event).

Tagliamento River site

The Cimano–Pinzano reach of the Tagliamento River (NE Italy) was selected for its structural and sedimentological similarities with many partly confined valleys such as in the Alpine foreland. The partly coarse, braided Tagliamento River is almost morphologically intact and constitutes a model reference for highly dynamic, natural rivers (Ward *et al.* 1999). This river is, too, characterized by a pluvio–nival regime that results in strong discharge fluctuations. At Venzone, 17 km upstream from the selected reach, the mean discharge is 90 m^3/s and the 100-year discharge is 4300 m^3/s. A detailed description of the morphology of this reach as well as a discussion on the impact of high-discharge events on the morphology are given in Huber and Huggenberger (2015).

The survey site is located on top of a flat gravel surface in an active zone at the lower part of the braided reach as shown in the aerial photograph in Fig. 3 (coordinates: 236,388; 5,118,308 WGS 1984 UTM 33N). There, the riverbed is about 350 m wide. From recent neotectonic structures, the reach is aggrading, although Huber and Huggenberger (2015) showed a more complex aggradation–degradation dynamic at a decadal timescale that depends on sediment supply, discharge and anthropogenic influence.

METHODOLOGY

Ground-penetrating radar data acquisition

At both sites, we collected ground-penetrating radar (GPR) data with a PulseEkko Pro GPR device (Sensors and Software, Inc., Mississagua, Ontario) with a pair of unshielded 100-MHz antennae separated by 1 m (constant offset). The antenna frequency was chosen to achieve a good trade-off

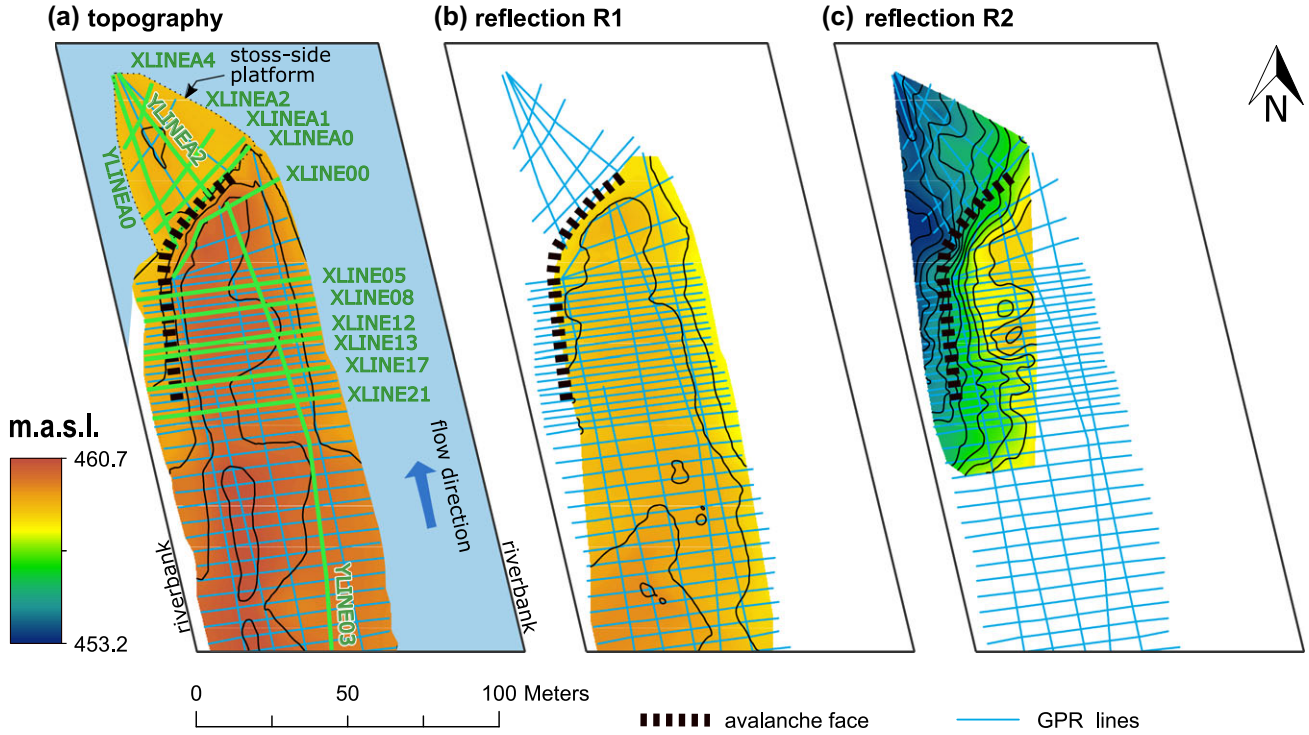

Figure 4 Site 1. (a) Surveyed topography of the gravel sheet and stoss-side platform. The blue area represents the part of the riverbed under water. (b) Elevation of reflection R1 (base of the gravel sheet). (c) Elevation of reflection R2 (erosional lower-bounding surface of the scour). The contours are traced every 0.5 m.

between imaging resolution and penetration depth required for stratigraphy analyses of gravel deposits. The sampling interval was set to 0.4 ns for the Alpine Rhine River site and 0.8 ns for the Tagliamento River site. An odometer allowed the recording of the GPR signal at regular spatial steps (0.25 m). The GPR profiles, the topography and the water edges (site 1) were surveyed with a total station (South, NTS 355L). The following nomenclature is adopted: GPR profiles parallel (perpendicular, respectively) to the general flow direction are called along-flow profiles (across-flow profiles, respectively).

Site 1. We collected 43 across-flow profiles and 5 along-flow profiles on a 200 × 60 m emerged part of a gravel sheet as shown in the survey map in Fig. 4(a). Furthermore, a smaller grid of 4 × 4 profiles (40 × 50 m) was recorded downstream the gravel sheet on the so-called stoss-side platform (Rice *et al.* 2009). Two common mid-point (CMP) data were recorded to estimate the mean electromagnetic wave velocity (Dix 1955; Tillard and Dubois 1995; Booth, Clark and Murray 2010). The water edge, shown in Fig. 4(a), indicates that the groundwater table lies between 0 and 1.3 m below the surface. Note the presence of a water stage gradient between both sides of the gravel sheet, that is, between backwater and river water.

Site 2. We collected 100 parallel across-flow profiles with 0.25-m trace spacing in both directions over a 25 × 50 m area on a flat gravel surface (Fig. 3). The high spatial sampling allowed horizontal slices of the data cube to be extracted. The horizontal slices were generated at different depths without vertical averaging because vertical averaging blurs the fine-scale structures. The horizontal slices enhance the three-dimensional continuity of the reflections by attenuating the impact of small profile misalignments.

Ground-penetrating radar data processing

The data are processed with the open-source software package RGPR (Huber and Hans 2018) following the processing workflow displayed in Table 1. The first seven processing steps aim to increase the signal-to-noise ratio and correct for low-frequency trends as well as amplitude attenuation. Then, to focus hyperbolic reflections to points and to correct the apparent slope of the reflections, a topographic Kirchhoff migration (Lehmann and Green 2000; Dujardin and Bano 2013) is applied with constant GPR wave velocity. The mean wave

Table 1 Processing of the ground-penetrating radar (GPR) data

Processing Step	Description/Literature
DC-shift removal	Remove constant amplitude shift
First-breaks picking and time-zero adjustment	E.g. Sabbione and Velis (2010).
Constant offset correction	Compensate for the 1-m-offset between transmitter and receiver antennae (the acquisition time of the traces is converted into the corresponding acquisition time for a mono-static antenna GPR).
Low-frequency trend removal (dewow)	Low-frequency trend estimated with a Hampel filter (e.g. Pearson 2002).
Band-pass frequency filtering	Remove the low and high noisy frequencies (corner frequencies: 5, 25, 150, 250 MHz).
Spherical and exponential amplitude corrections	Compensate for geometric spreading and attenuation of the GPR signal (e.g. Kruse and Jol 2003; Grimm *et al.* 2006). Exponential attenuation coefficient: 0.035 m^{-1} (0.30 dB/m).
2D median filtering	Applied over a 3-by-3 neighbourhood to remove high-frequency noise.
Topographic Kirchhoff migration	Topographic Kirchhoff migration (Lehmann and Green 2000; Dujardin and Bano 2013) with a constant GPR wave velocity (0.1 m/ns) that leads to results that are accurate enough for the purpose of the study.
Automatic gain control gain	Amplify weaker reflection (0.25 m standard deviation).

velocity is estimated from a coherency analysis of the CMP data (Booth *et al.* 2010). An automatic gain control is then applied to amplify weaker reflection. We do not focus on amplitude variations because they are very difficult to interpret in heterogeneous deposits.

The use of a constant wave velocity for data migration is an approximation that leads to results that are accurate enough for the purpose of this study. Even with a velocity model where the velocity varies with depth, uncertainties arise from the horizontal layer assumptions in CMP analysis and migration as well as from the constant, lateral velocity assumption in migration (because we have CMP data only at one location). According to Cassidy (2009), the uncertainty of the velocity estimated from CMP is about ±10% or worse (see also Tillard and Dubois 1995). We agree with Cassidy when he states that 'it is not worth wasting time trying to get a highly accurate velocity–depth profile when a constant, average velocity for all depths will produce the same interpretational results' (Cassidy 2009). Our aim is not to quantify with high accuracy the subsurface structures but to identify the main sedimentary structures and to relate them to the morphology. We estimate the uncertainty of the reflection depth to be ± 0.5 m. Such an uncertainty has no impact on the main study conclusions. However, accuracy would be required for further systematic GPR investigations on scour size distribution that would need a significant number of observations.

Ground-penetrating radar data interpretation

The interpretation of GPR data is an educated guess based on the basic principles of GPR facies analyses (Beres and Haeni 1991) and on knowledge gained from the comparison of GPR data with outcrop observations in gravel pits (Huggenberger 1993; Beres *et al.* 1995, 1999; Huggenberger *et al.* 1998). The following fundamental rules guide the interpretation of GPR data: (i) continuity of the dominant reflections, (ii) differences in reflection patterns and (iii) angular unconformity between reflection patterns (Huber and Huggenberger 2016).

For the Alpine Rhine River data, reflections on the along-flow profiles are first picked. Then, the picked reflections are compared with the across-flow profile and corrected if necessary. These steps are iterated until the interpretation is coherent with both the along-flow and across-flow profile. For the Tagliamento River data, reflections are picked on the depth slices. For the sake of a reliable inference, only non-ambiguous structures are interpreted. The picked reflections are then interpolated to surfaces in GOCAD (Paradigm) based on the discrete smooth interpolation (Mallet 1989, 1992), a well-established interpretation method in geology that minimizes a fairness criterion (the squared discrete Laplacian).

RESULTS

Ground-penetrating radar data

The wave velocities vary between 0.085 and 0.115 m/ns and are comparable with those of earlier findings in similar sediments (e.g. Beres *et al.* 1999). In the upper 4 to 5 m, higher wave velocities (0.105–0.115 m/ns) are observed, while in the lower part the velocities range between 0.085 and 0.095 m/ns. Note that the velocity change is not related to the groundwater table that lies 0 to 1.3 m below the surface.

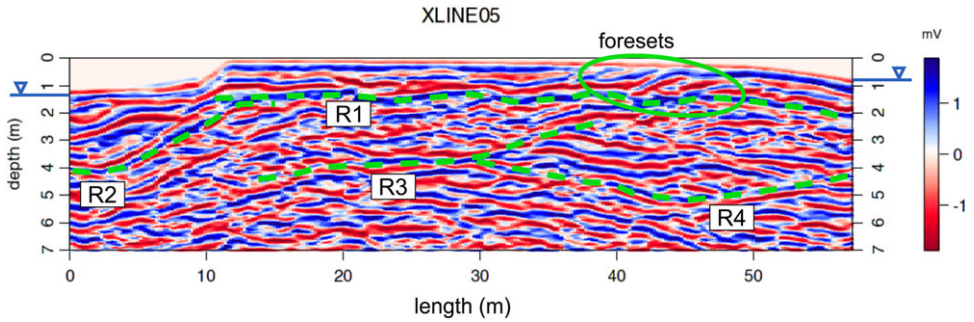

Figure 5 Site 1. Ground-penetrating radar profile XLINE05 with interpretation (the position of XLINE05 is indicated in Fig. 4). The profile elevation is 460.18 m.a.s.l. The water stage is denoted with the small upside-down triangles on the left and right sides of the profile.

Only a selection of the many recorded GPR profiles is presented for illustration purposes. In general, the reflections on the across-flow profiles are much less continuous than the reflections on the along-flow profiles that display rather continuous low-angle reflections. This marked difference in the reflection patterns between across-flow and along-flow profiles results from the interplay between the anisotropic sedimentary structures and the asymmetric antenna radiation pattern and illustrates the difficulty to correctly interpret two-dimensional GPR data.

Alpine Rhine River ground-penetrating radar data

The up to 2-m-thick gravel sheet has a sharp avalanche face at its downstream edge towards the riverbank. The avalanche face orientation indicates the direction of the most recent gravel sheet migration (Fig. 4a). The stoss-side platform downstream from the gravel sheet is completely flat and consists of fine sediments, mainly sand. Below the gravel sheet, a strong horizontal, continuous reflection is discordant with the reflections below. This reflection, denoted R1 in the GPR data shown in Figs 5 and 7, is identified as the gravel sheet base that presumably consists in an armour layer. Note that reflection R1 cannot be related to the groundwater table that clearly lies 1 m above. We could not identify a reflection from the groundwater table, most probably because the ratio of the capillary fringe thickness to the wave length is more than 0.3 (Annan, Cosway and Redman 1991; Bano 2006). A significant capillary fringe is indeed expected because the fine sediments of the Rhine deposits have a high capillarity (Bear 1972) and the river stage varies over 0.5 m twice a day due to hydropeaking.

Another horizontal reflection, that is partially visible between R1 and the top of the gravel sheet, suggests that the gravel sheet consists, in fact, of two superimposed layers (the reflection immediately below the forests in Fig. 7). In the upper layer, short, inclined reflections oriented at −45° with respect to the general flow direction are visible (this horizontal orientation is estimated from the apparent inclination of the reflections on the along-flow and across-flow profiles, see Fig. 7). These inclined reflections can be interpreted as foresets that resulted from the migration or climbing of the upper gravel sheet over the lower gravel sheet. The foreset orientation that is consistent with the avalanche face orientation supports this interpretation. The top of the climbing gravel sheet may have been partially eroded as indicated by the decreasing size of the foresets as well as the decreasing thickness of the upper layer towards the left riverbank. The apparent propagation length inferred from the preserved foresets is about 15 m and corresponds to the minimum expected migration length.

A strongly dipping reflection at the downstream end of the gravel sheet (reflection R2 in Figs 4, 5, 6 and 8) is discordant with the reflection pattern below and is therefore identified as the erosional lower-bounding surface of a scour. The imaged part of this erosional surface is about 30 × 100 m large and 4.5 ± 0.5 m deep (7.4 ± 0.5 m deep relative to the maximum elevation of the gravel sheet) and is located at the expected scour position shown in Fig. 1(c). The erosional surface already starts to dip 10 to 15 m upstream from the avalanche face (i.e. below the gravel sheet; Fig. 4c). This spatial overlap between the scour and the gravel sheet implies that the gravel sheet migrated over the scour while it was already filled. The reflections within the lower part of the scour are curved and concave, exhibiting an onion-like pattern (Fig. 8). Such a pattern can result from sediment progradation within the scour. The up to 2-m-thick horizontal reflections observed on top of the scour (Fig. 6) can correspond to layers of fine sediments that were deposited in the partially filled scour at low discharge.

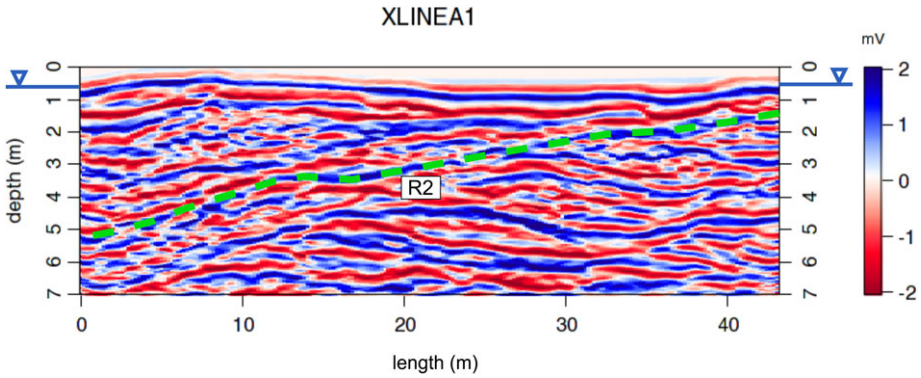

Figure 6 Site 1. Ground-penetrating radar profile XLINEA1 with interpretation (the position of XLINEA1 is indicated in Fig. 4). The profile elevation is 459.03 m.a.s.l. The water stage is denoted with the small upside-down triangles on the left and right sides of the profile.

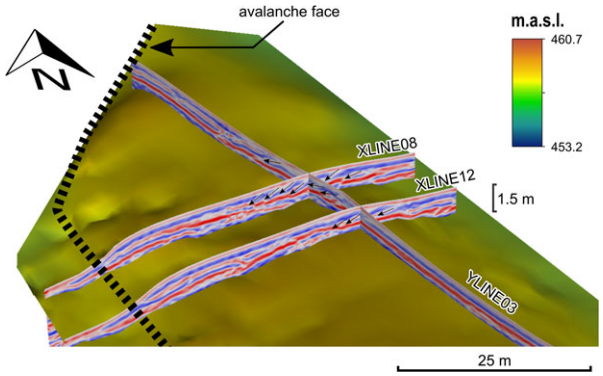

Figure 7 Site 1. Elevation of reflection R1 (base of the gravel sheet). The foresets on the ground-penetrating radar data are indicated by a series of black arrows.

Other small erosional lower-bounding surfaces (<50 × 50 m and about 2.1 to 2.7 m deep) were identified at approximately 3 to 6 m below the gravel sheet (e.g. reflections R3 and R4 in Fig. 5). Their original depths and extents are highly uncertain as well as their origins. These erosional lower-bounding surfaces can originate from the channelized Alpine Rhine River or from the former Alpine Rhine River prior to the channelization.

Tagliamento River ground-penetrating radar data

On the across-flow profiles of the Tagliamento River data, a more than 30-m-large scour is identified by the lower and upper reflections R1 and R2 as well as by the marked angular unconformity between the reflections within R1 and R2 and the reflections around (Fig. 9). The angular unconformity strongly suggests that the lower reflection R1 is an erosional lower-bounding surface. The curved reflections between R1 and R2 that merge tangentially with the lower reflection R1 and dips towards the north can be, therefore, interpreted as scour cross-beds (compare Figs 3 and 8). On top of the scour (i.e. above reflection R2), continuous, horizontal reflections dominate and form an up to 2-m-thick unit that is interpreted as a gravel sheet remnant. The reflections outside the scour are rather sub-horizontal and occasionally discontinuous and therefore hardly interpretable.

The fence diagram in Fig. 10(a) illustrates the relationship between the vertical and horizontal GPR information. The inclined reflections on across-flow profiles are visible on the horizontal slice as a stripe pattern that contrasts with the less distinct pattern around. The surface of the lower reflection R1 (Figs 10b and 11a) is spoon-shaped, 2.5 m deep, 20 m wide and more than 30 m long. The long axis of the scour has an angle of 50° with the general flow direction.

Within the scour, six inclined almost planar cross-beds are identified (Fig. 10b). They are parallel to the horizontal length axis of the scour with a spacing of 2 to 5 m. The cross-beds merge tangentially with the lower reflection R1 and their dip angle decreases from approximately 50° to 30° from south-east to north-west. Note that the tangential pattern of the reflections within the scour was strongly attenuated by the delineation and interpolation process (compare the GPR data in Fig. 9 with the three-dimensional structure model in Fig. 10b). Along the main scour axis, the internal reflections are rather sub-horizontal, making the identification of such scour structures by GPR surveys along this direction challenging. At a depth of about 4 m, there is a change in the orientation of the low-angle dipping reflections outside the scour.

DISCUSSION

Ground-penetrating radar data interpretation uncertainties

Three main types of uncertainties impact the workflow of this study, from the data acquisition to the interpretation

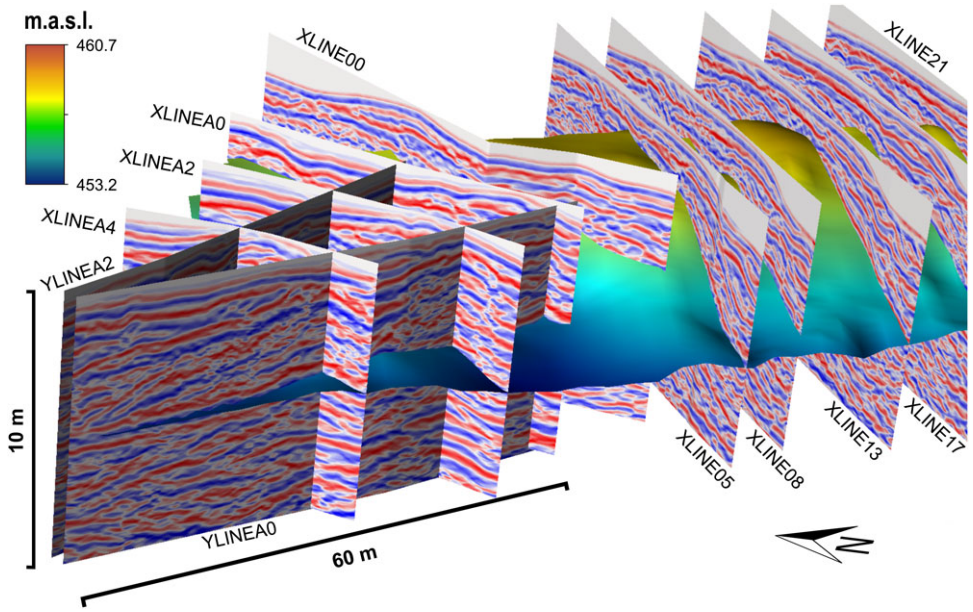

Figure 8 Site 1. Elevation of reflection R2 (erosional lower-bounding surface of the scour) with ground-penetrating radar data.

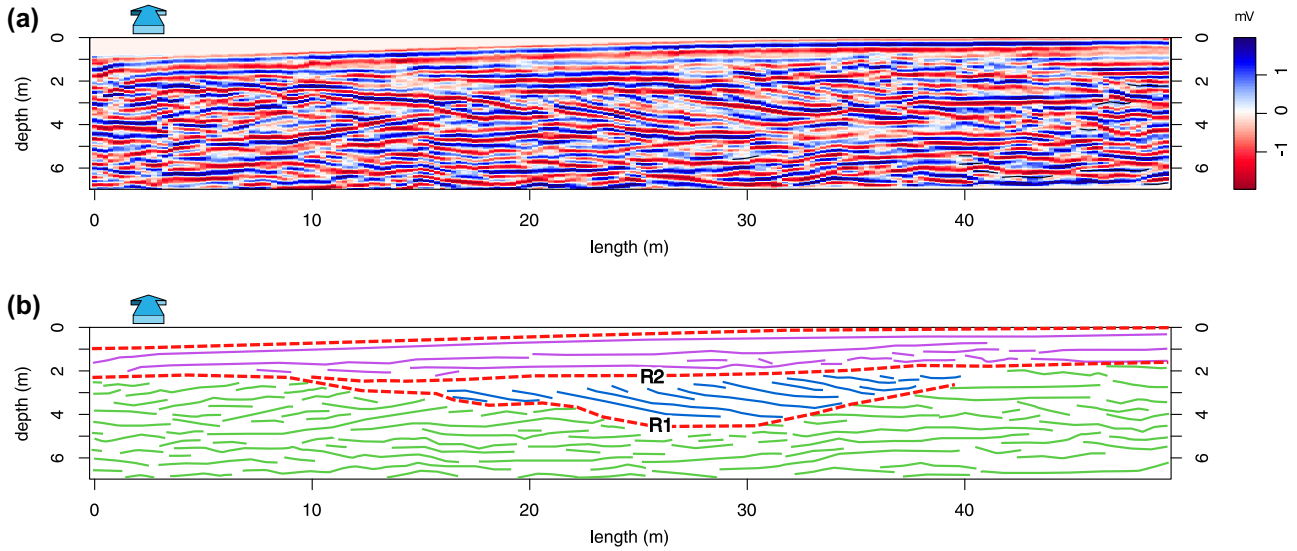

Figure 9 Site 2. (a) Ground-penetrating radar data located 2.5 m from the downstream end of the ground-penetrating radar grid. (b) Interpretation of (a). The red dashed lines indicate the boundaries between the interpreted units. The blue arrows indicate the general flow direction.

of the interpolated surfaces: (i) the 'depthing' (as opposed to imaging) uncertainty related to uncertain data acquisition (e.g. positioning), data processing (e.g. assumptions violated in practices) and reflector picking (e.g. where to pick the reflections on the wavelet); (ii) the conceptual uncertainty, that is, 'the range of concepts that geoscientists could apply to a single data set' (Bond *et al.* 2007); (iii) the interpretation uncertainty, that is, the way how the picked reflections correspond to the true geological structure. This uncertainty directly depends on the conceptual uncertainty (Bond 2015).

The depthing uncertainty, which has no significant impact on the interpretational study results, can be quantified within a probability framework by combining ground-penetrating radar (GPR) data simulation with prior probability distributions on data acquisition, data processing

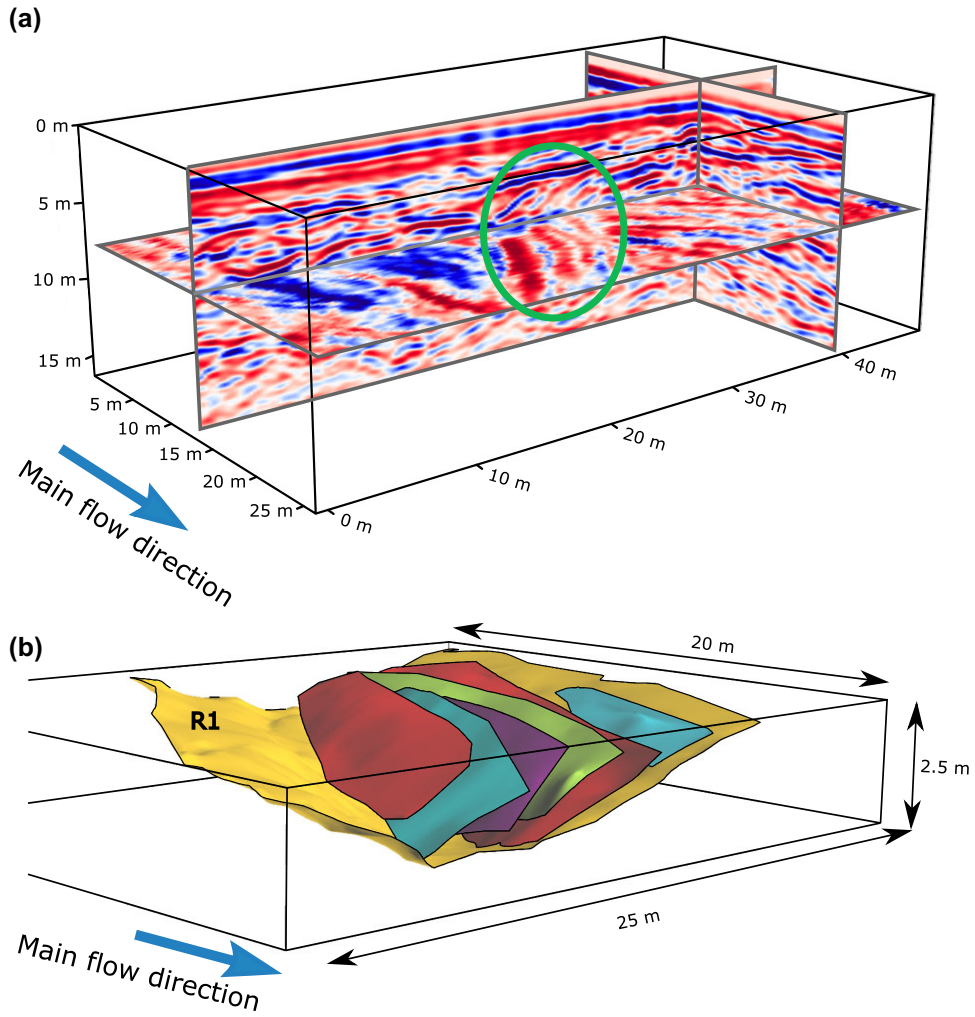

Figure 10 Site 2. (a) Two vertical ground-penetrating radar profiles and one horizontal slice. The green circle indicates the position of the inclined, curved reflections within the scour structure. (b) Surfaces resulting from the delineation and interpolation of the depth slices.

and reflector picking. Such an uncertainty quantification is beyond the scope of this paper. The two other types of uncertainties are much more difficult to evaluate and can have a much stronger impact on the study results. The degree of conceptual and interpretation uncertainty mainly depends on 'elicit[ing] intelligent information while mitigating against the unconscious negative use of prior knowledge' (Bond *et al.* 2007). Education and three-dimensional imaging are the key to reduce these two uncertainties.

Note that our approach relies on a hypothesis-testing workflow for the Alpine Rhine River data, where the picked reflectors on a profile are compared with the picked reflections on the adjacent reflections. For the Tagliamento River data, only the unambiguous reflections are picked on the horizontal slices that integrate three-dimensional information. Furthermore, the fundamental interpretation rules (see the section 'Ground-penetrating radar data interpretation') used to pick the reflections are a guaranty against inconsistencies. Moreover, we deliberately renounce to pick and interpret inconsistent or unclear reflections. The interpretation of the GPR data is based on several studies that compared GPR data with observations of vertical exposures in gravel carries (e.g. Huggenberger 1993; Huggenberger *et al.* 1994; Beres *et al.* 1995, 1999; Asprion and Aigner 1997, 1999; Heinz and Huggenberger *et al.* 1998; Heinz and Aigner 2003; Kostic and Aigner 2007; Bayer *et al.* 2011). For all these reasons, the study results can be regarded as reliable and robust.

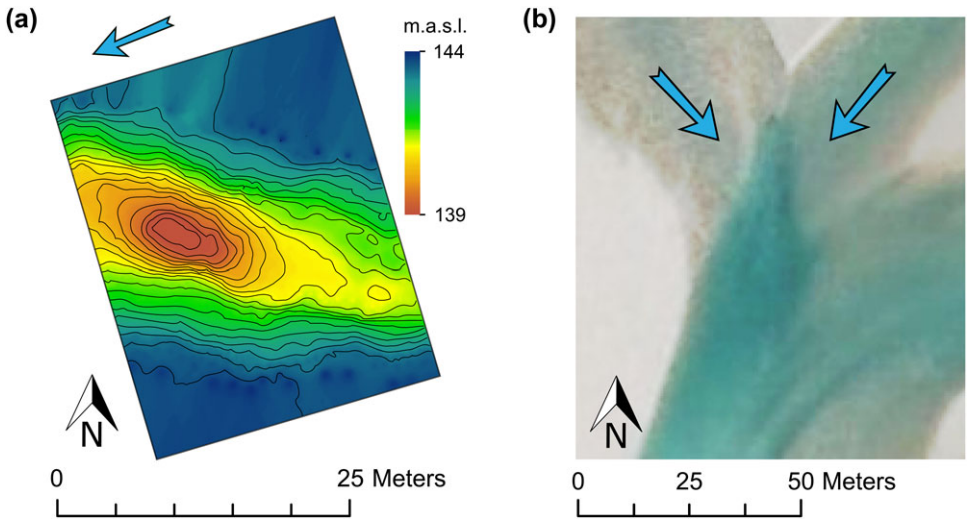

Figure 11 Site 2. (a) Elevation map of the lower reflection R1; the contours are traced every 0.25 m, and the blue arrow indicates the general flow direction. (b) Confluence scour in the studied reach of the Tagliamento River in 2011 (orthophoto from the Autonomous Region of Friuli Venezia Giulia). The blue arrows indicate the flow directions.

Discrepancy between riverbed morphology and near subsurface

The study findings corroborate previous research on gravel sheets and associated scours (Ashmore 1982; Jäggi 1984; Ikeda 1984; Siegenthaler and Huggenberger 1993; Pyrce and Ashmore 2003; Huggenberger and Regli 2006; Bankert and Nelson 2018) and demonstrate the potential of GPR for research on scour fills. Furthermore, by highlighting the presence of deep, buried scours the study findings confirm that the surface morphology is not representative of the sedimentary structures (see Huber and Huggenberger 2015).

In consequence, riverbed bathymetric surveys can underestimate the real scour depths up to a few metres. Jäggi (1983) and Adami *et al.* (2016) analysed cross-section measurements of the riverbed of the Alpine Rhine River acquired between 23.8 and 60.8 km in 1972–1981 and 2005, respectively (cross-sections with an average spacing of 200 m). On average, the scour depth estimated by Jäggi was about 3.5 m with a maximum of 4.44 m, while Adami *et al.* estimated the riverbed elevation difference to range between 2.5 and 4 m. In contrast, the partially imaged scour of the Alpine Rhine River is 4.5 ± 0.5 m deep, and the elevation difference between scour bottom and gravel sheet is 7.4 ± 0.5 m. Because the scour is manifestly much larger and deeper than its imaged part, these two values must be considered as the lower limits of scour depth and riverbed elevation range. It is therefore critical to account for the bias of bathymetric surveys when designing flood protection against river embankment failures.

Another consequence arising from the difference between riverbed morphology and subsurface is that subsurface models of gravel-bed river deposits cannot be solely based on the riverbed morphology. Subsurface models based on the stacking of individual riverbed morphologies (e.g. Webb 1995; Pirot, Straubhaar and Renard 2014) underestimate scour fill deposits that strongly impact subsurface flow and transport because of their generally highly permeable lithologies with regard to the other coarse, braided river deposits (Jussel *et al.* 1994; Huber and Huggenberger 2016).

Scouring processes

The scour fills presented in this study were produced by different formative processes, although the sediment sorting processes are comparable. In the case of the Alpine Rine River, the two concordant layers within the gravel sheet as well as the foresets indicate that gravel sheet can migrate longitudinally, at least over short distance, through the accretion of single gravel sheets on top of each other. But other migration mechanisms such as full transport (Todd 1989) are possible at high discharge. The vertical growth of gravel sheets modifies the roughness of the riverbed that increases the flow turbulence (e.g. the inrush activity). This flow turbulence combined with the flow diversion exerted by the slight inclination of the gravel sheets towards one of the riverbanks induces the scouring of the riverbed downstream from the gravel sheet.

The scour fill of the Tagliamento River is a typical example of coarse, braided river deposits. These sedimentary structures were intensively discussed in the literature and generally consist of open-framework–bimodal gravel couplet cross-beds covered by a layer of poorly sorted gravel (e.g. Siegenthaler and Huggenberger 1993; Huggenberger and Regli 2006). Such scour fills can originate either from low-discharge confluences or from flow confluence induced by gravel sheets at high discharge. The imaged scour closely resembles in terms of shape and size to a low-discharge confluence observed in 2011 in the same reach of the Tagliamento River, as shown in the aerial photograph in Fig. 11(b) (to be compared with Fig. 11a). The scour cross-beds can result from the lateral scour migration and filling.

Directions for further research

Scours can threaten riverbank stability and are therefore highly relevant for the design of flood protection embankments. However, the relationship between scour depth and flood event peak and duration is extremely challenging because of the still limited knowledge on how gravel sheets and scours form and migrate (Huber and Huggenberger 2015). The analysis of Landsat images and discharge records of the Alpine Rhine River could not reveal a clear relationship between gravel sheet migration and peak discharge and duration (Adami *et al.* 2016). Furthermore, the position of the gravel sheets could also depend on the aggradation–degradation dynamic that does not occur uniformly but generally alternates between the left and right river sides.

Systematic investigations combining GPR measurements with morphological observations (e.g. aerial photograph, satellite imagery, LiDAR measurements) are the key to gaining knowledge on the sedimentary processes related to scours. We highly recommend to repeat GPR measurements before and after high-discharge events to quantify river scouring. The inferred near-subsurface dynamics of the riverbed could be put into relation with the discharge peak and duration as well as with the gravel sheet dynamics. Furthermore, repeated GPR measurements can significantly strengthen the GPR data interpretation, that is, reduce the conceptual and interpretation uncertainties, because the interpretation would focus on changes of reflection patterns that could be related to discharge event. A major challenge that still remains untackled is the measurement of riverbed topography as well as the imaging of near-subsurface structures at high discharge (i.e., through turbid and turbulent flows). These measurements would directly reveal the dynamics of the sedimentary processes.

CONCLUSION

This work demonstrates how ground-penetrating radar (GPR) studies can contribute to better flood protection measures through a deeper appreciation of the sedimentological processes. The GPR data, collected on the riverbed of a reach of the Alpine Rhine River with alternate gravel sheets, showed the presence of a more than 4.5 m deep scour close to the riverbank, downstream the gravel sheet. Another GPR survey on the riverbed of the braided Tagliamento River illustrates the three-dimensional structure of confluence scour found in braided river deposits. Bathymetric measurements cannot assess the depth of such filled scours, and therefore they tend to underestimate the maximal scour depth, a critical parameter for flood embankment design. The data from the Alpine Rhine River indicated that the alternate gravel sheet migrated 15 m downstream over the filled scour. This distance is far below the maximal migration distance (up to 300 m) observed by Adami *et al.* (2016).

As demonstrated in this study, excellent knowledge of the sedimentology of gravel-bed river systems appreciably contributes to a better interpretation of the GPR data that, however, still remain unequivocal up to some extent. The present findings should stimulate the combined use of GPR measurements, flume experiments and numerical modelling of the dynamics of river systems to gain a better understanding of these systems and quantify the impact of riverbed scouring on the surface water–groundwater interaction as well as on benthic macroinvertebrate abundance.

ACKNOWLEDGEMENTS

Work by the first author was partially funded by the Swiss National Science Foundation (grant no. P2BSP2_161955). We thank the Rheinunternehmen (Canton St. Gallen) for the authorization to collect GPR data on the Alpine Rhine River bed and Lukas Egli for helping with the GPR data acquisition. We thank both Sajad Jazayeri and an anonymous reviewer whose comments helped improve and clarify this manuscript. The authors have no conflict of interest to declare.

REFERENCES

Adami L., Bertoldi W. and Zolezzi G. 2016. Multidecadal dynamics of alternate bars in the Alpine Rhine River. *Water Resources Research* **52**, 8938–8955.

Annan A.P., Cosway S.W. and Redman J.D. 1991. Water table detection with ground-penetrating radar. *Meeting of the Society of Exploration Geophysicists* **61**, 494–496.

Ashmore P.E. 1982. Laboratory modelling of gravel braided stream morphology. *Earth Surface Processes and Landforms* **7**, 201–225.

Ashmore P.E. 1985. *Process and form in gravel braided streams: Laboratory modelling and field observations*. PhD thesis, University of Alberta, 414 pp.

Ashmore P. and Gardner J.T. 2008. Unconfined confluences in braided rivers. In: *River Confluences, Tributaries and the Fluvial Network* (eds S.P. Rice, A.G. Roy and B.L. Rhoads), pp. 119–147. John Wiley & Sons, Ltd.

Ashmore P. and Parker G. 1983. Confluence scour in coarse braided streams. *Water Resources Research* **19**,392–402.

Asprion U. and Aigner T. 1997. Aquifer architecture analysis using ground-penetrating radar: Triassic and Quaternary examples (S. Germany). *Environmental Geology* **31**, 66–75.

Asprion U. and Aigner T. 1999. Towards realistic aquifer models: Three-dimensional georadar surveys of Quaternary gravel deltas (Singen Basin, SW Germany). *Sedimentary Geology* **129**, 281–297.

Bankert A.R. and Nelson P.A. 2018. Alternate bar dynamics in response to increases and decreases of sediment supply. *Sedimentology* **64**, 702–720.

Bano M. 2006. Effects of the transition zone above a water table on the reflection of GPR waves. *Geophysical Research Letters* **33**, L13309.

Bayer P., Huggenberger P., Renard P. and Comunian A. 2011. Three-dimensional high resolution fluvio-glacial aquifer analog: Part 1: Field study. *Journal of Hydrology* **405**, 1–9.

Bear J. 1972. *Dynamics of Fluids in Porous Media*, pp. 764. Elsevier, New York.

Beres M., Green A.G., Huggenberger P. and Horstmeyer H. 1995. Mapping the architecture of glaciofluvial sediments with three-dimensional georadar. *Geology* **23**, 1087–1090.

Beres M. and Haeni F.P. 1991. Application of ground-penetrating-radar methods in hydrogeologie studies. *Groundwater* **29**, 375–386.

Beres M., Huggenberger P., Green A.G. and Horstmeyer H. 1999. Using two- and three-dimensional georadar methods to characterize glaciofluvial architecture. *Sedimentary Geology* **129**, 1–24.

Best J.L. 1993. On the interactions between turbulent flow structure, sediment transport and bedform developments: Some considerations from recent experimental research. In: *Turbulence: Perspectives on Flow and Sediment Transport* (eds N.J. Clifford, J.R. French and J. Hardisty), pp. 61–93. John Wiley & Sons, Ltd, Chichester, UK.

Bond C.E. 2015. Uncertainty in Structural Interpretation: Lessons to be learnt. *Journal of Structural Geology* **74**, 185–200.

Bond C.E., Gibbs A.D., Shipton Z.K. and Jones S. 2007. What do you think this is? "Conceptual uncertainty" in geoscience interpretation. *GSA Today* **17**, 4–10.

Booth A.D., Clark R. and Murray T. 2010. Semblance response to a ground-penetrating radar wavelet and resulting errors in velocity analysis. *Near Surface Geophysics* **8**, 235–246.

Cassidy. 2009. Chapter 5 – Ground penetrating radar data processing, modelling and analysis. In: *Ground Penetrating Radar Theory and Applications* (ed. H.M. Jol), pp. 141–176. Elsevier, Amsterdam.

Claude N., Rodrigues S., Bustillo V., Bréhéret J.-G., Tassi P. and Jugé P. 2014. Interactions between flow structure and morphodynamic of bars in a channel expansion/contraction, Loire River, France. *Water Resources Research* **50**, 2850–2873.

Dam R.L.V. and Schlager W. 2000. Identifying causes of ground-penetrating radar reflections using time-domain reflectometry and sedimentological analyses. *Sedimentology* **47**, 435–449.

Davis J.L. and Annan A.P. 1989. Ground-penetrating radar for high-resolution mapping of soil and rock stratigraphy. *Geophysical Prospecting* **37**, 531–551. https://doi.org/10.1111/j.1365-2478.1989.tb02221.x

Dujardin J.-R. and Bano M. 2013. Topographic migration of GPR data: Examples from Chad and Mongolia. *Comptes Rendus Geoscience* **345**, 73–80.

Dix C.H. 1955. Seismic velocities from surface measurements. *Geophysics* **20**, 68–86.

Grebenau H. 1870. Der Rhein vor und nach seiner Regulierung auf der Strecke von der Lauter bis Germersheim, XXVIII. und XXIX. Jahresbericht der Pollichia, eines naturwissenschaftlichen Vereines der Rheinpfalz, Dürkheim a.d.H.

Grimm R.E., Heggy E., Clifford S., Dinwiddie C., McGinnis R. and Farrell D. 2006. Absorption and scattering in ground-penetrating radar: Analysis of the Bishop Tuff. *Journal of Geophysical Research* **111**, E06S02.

Guillaume J.H.A., Hunt R.J., Comunian A., Blakers R.S. and Fu B. 2016. Methods for exploring uncertainty in groundwater management predictions. In: *Integrated Groundwater Management*, pp. 711–737. Springer International Publishing.

Heinz J. and Aigner T. 2003. Three-dimensional GPR analysis of various Quaternary gravel-bed braided river deposits (southwestern Germany). *Geological Society, London, Special Publications* **211**, 99–110.

Huber E., Anders B. and Huggenberger P. 2018. Quantifying scour depth in a straightened gravel-bed river with ground-penetrating radar. 17th International Conference on Ground Penetrating Radar (GPR). *Rapperswil* **2018**, 1–4.

Huber E. and Hans G. 2018. RGPR — An open-source package to process and visualize GPR data. *17th International Conference on Ground Penetrating Radar*, Switzerland, Rapperswil, 18–21 June 2018, pp. 1–4.

Huber E. and Huggenberger P. 2015. Morphological perspective on the sedimentary characteristics of a coarse, braided reach: Tagliamento River (NE Italy). *Geomorphology* **248**, 111–124.

Huber E. and Huggenberger P. 2016. Subsurface flow mixing in coarse, braided river deposits. *Hydrology and Earth System Sciences* **20**, 2035–2046.

Huggenberger P. 1993. Radar facies: Recognition of facies patterns and heterogeneities within Pleistocene Rhine gravels, NE Switzerland. *Geological Society, London, Special Publications* **75**, 163–176.

Huggenberger P., Hoehn E., Beschta R. and Woessner W. 1998. Abiotic aspects of channels and floodplains in riparian ecology. *Freshwater Biology* **40**, 407–425.

Huggenberger P., Meier E. and Pugin A. 1994. Ground-probing radar as a tool for heterogeneity estimation in gravel deposits: Advances in

data-processing and facies analysis. *Journal of Applied Geophysics* **31**, 171–184.

Huggenberger P. and Regli C. 2006. A sedimentological model to characterize braided river deposits for hydrogeological applications. In: *Braided Rivers: Process, Deposits, Ecology and Management* (eds G.H. Sambrook Smith, J.L. Best, C.S. Bristow and G.E. Petts), pp. 51–74. Blackwell Publishing Ltd, Oxford, UK.

Hundey E.J. and Ashmore P.E. 2009. Length scale of braided river morphology. *Water Resources Research* **45**, W08409.

Ikeda S. 1984. Prediction of alternate bar wavelength and height. *Journal of Hydraulic Engineering* **110**, 371–386.

Jäggi M. 1983. Alternierende Kiesbänke (Alternate bars), PhD thesis, Swiss Federal Institute of Technology Zurich, Diss. ETH Nr. 7208. Switzerland, pp. 286.

Jäggi M. 1984. Formation and effects of alternate bars. *Journal Hydraulic Engineering* **110**, 142–156.

Jussel P., Stauffer F. and Dracos T. 1994. Transport modeling in heterogeneous aquifers: 1. Statistical description and numerical generation of gravel deposits. *Water Resources Research* **30**, 1803–1817.

Kleinhans M.G. and van den Berg J.H. 2011. River channel and bar patterns explained and predicted by an empirical and a physics-based method. *Earth Surface Processes and Landforms* **36**, 721–738.

Kostic B. and Aigner T. 2007. Sedimentary architecture and 3D ground-penetrating radar analysis of gravelly meandering river deposits (Neckar Valley, SW Germany). *Sedimentology* **54**, 789–808.

Kruse S. and Jol H.M. 2003. Amplitude analysis of repetitive GPR reflections on a Lake Bonneville Delta, Utah. In: *GPR in Sediments, Geological Society of London*, Vol. **211** (eds C.S. Bristow and H.M. Jol), pp. 287–298. Geological Society, London, Special Publication.

Lehmann F. and Green A.G. 2000. Topographic migration of georadar data. Proc. SPIE 4084, Eighth International Conference on Ground Penetrating Radar, pp. 5.

Mallet J.L. 1989. Discrete smooth interpolation in geometric modeling. *ACM-Transactions on Graphics* **8**, 121–144.

Mallet J.L. 1992. Discrete smooth interpolation. *Computer Aided Design Journal* **24**, 263–270.

Marti C. and Bezzola G.R. 2005. Braided gravel-bed rivers with a limited width: Preliminary results of a hydraulic model study. In: *Fluvial Sedimentology VII* (eds I. Jarvis, M.D. Blum, S.B. Marriott and S.F. Leclair), pp. 135–144. International Association of Sedimentologists.

Mosley M. 1976. An experimental study of channel confluences. *The Journal of Geology* **84**, 835–562.

Neal A. 2004. Ground-penetrating radar and its use in sedimentology: principles, problems and progress. *Earth-Science Reviews* **66**, 261–330.

Nearing G.S., Tian Y., Gupta H.V., Clark M.P., Harrison K.W. and Weijs S.V. 2016. A philosophical basis for hydrological uncertainty. *Hydrological Sciences Journal* **61**, 1666–1678.

Parker G. 1976. On the cause and characteristic scales of meandering and braiding in rivers. *Journal of Fluid Mechanics* **76**, 457–480.

Pearson R.K. 2002. Outliers in process modeling and identification. *IEEE Transactions on Control Systems Technology* **10**, 55–63.

Pirot G., Straubhaar J. and Renard P. 2014. Simulation of braided river elevation model time series with multiple-point statistics. *Geomorphology* **214**, 148–156.

Pyrce R.S. and Ashmore P.E. 2003. Particle path length distribution in meandering gravel-bed streams: Results from physical models. *Earth Surface Processes and Landforms* **28**, 951–966.

Rice S.P., Church M., Wooldridge C.L. and Hickin E.J. 2009. Morphology and evolution of bars in a wandering gravel-bed river; lower Fraser river, British Columbia, Canada. *Sedimentology* **56**, 709–736.

Sabbione J.I. and Velis D. 2010. Automatic first-breaks picking: New strategies and algorithms. *Geophysics* **75**, 67–76.

Salter T. 1993. Fluvial scour and incision: Models for their influence on the development of realistic reservoir geometries. *Geological Society, London, Special Publications* **73**, 33–5.

Siegenthaler C. and Huggenberger P. 1993. Pleistocene Rhine gravel: deposits of a braided river system with dominant pool preservation. In: *Braided Rivers, Geological Society*, Vol. **75** (eds J.L. Best and C.S. Bristow). pp. 147–162. Special Publications, London.

Storz-Peretz Y. and Laronne J.B. 2013. Morphotextural characterization of dryland braided channels. *GSA Bulletin* **125**, 1599–1617.

Tillard S. and Dubois J.-C. 1995. Analysis of GPR data: wave propagation velocity determination. *Journal of Applied Geophysics* **33**, 77–91.

Todd S.P. 1989. Stream-driven, high-density gravelly traction carpets: possible deposits in the Trabeg Conglomerate Formation, SW Ireland and some theoretical considerations of their origin. *Sedimentology* **36**, 513–530.

Ward J., Tockner K., Edwards P., Kollmann J., Bretschko G., Gurnell A., *et al.* 1999. A reference river system for the Alps: The 'Fiume Tagliamento'. *Regulated Rivers: Research & Management* **15**, 63–75.

Webb E.K. 1995. Simulation of braided channel topology and topography. *Water Resources Research* **31**, 2603–2611.

Zarn B. 2008. Development concept river Alpine Rhine. *Österreichische Wasser- und Abfallwirtschaft* **60**, 81, Heft 05–06/2008.